Journal of Hepatocellular Carcinoma Dovepress

Open Access Full Text Article ORIGINAL RESEARCH

# Yiqi Liangxue Jiedu Prescription Inhibited the Canonical Wnt Pathway to Prevent Hepatocellular Precancerous Lesions

Yuling Liang[1,*], Yuqing Xie[1,*], Zhibo Dang[2,*], Mengge Li[3,*], Lihua Yu[1], Xinhui Wang[4], Peng Wang[5], Zhiyun Yang[1]

[1]Center of Integrative Medicine, Beijing Ditan Hospital, Capital Medical University, Beijing, People's Republic of China; [2]Ethics Committee Office, Henan Province Hospital of TCM, Henan, People's Republic of China; [3]Department of Hepatobiliary Spleen and Stomach, Henan Province Hospital of TCM, Henan, People's Republic of China; [4]Beijing Children's Hospital, Capital Medical University, Beijing, People's Republic of China; [5]Department of Pathology, Beijing Ditan Hospital, Capital Medical University, Beijing, People's Republic of China

*These authors contributed equally to this work

Correspondence: Peng Wang, Department of Pathology, Beijing Ditan Hospital, Capital Medical University, Beijing, 100015, People's Republic of China, Tel +86-10-84322530, Email dtpengwang@163.com; dtwangpeng@mail.ccmu.edu.cn; Zhiyun Yang, Center of Integrative Medicine, Beijing Ditan Hospital, Capital Medical University, Beijing, 100015, People's Republic of China, Tel +86-10-84,322,148, Email yangzhiyun2016@163.com

**Purpose:** Yiqi Liangxue Jiedu prescription (YLJP), a Chinese medicine that is commonly used to prevent liver cancer and is authorized by a national patent (patent No. ZL202110889980.5) has a therapeutic effect on precancerous lesions; however, the underlying mechanism remains unclear. This study is aimed at determining the clinical therapeutic efficacy of YLJP in patients with precancerous liver lesions and to explore and validate its possible effector mechanism.

**Patients and Methods:** The 1-year incidence of hepatocellular carcinoma (HCC) was retrospectively analyzed in 241 patients with cirrhosis complicated by abnormal alpha-fetoprotein precancer. Network pharmacological analysis, molecular docking, and molecular dynamics simulation were used to explore the key targets and compounds of YLJP in treating HCC. Immunohistochemical methods were used to detect the expression of key proteins in tumor and cirrhotic tissues. Finally, the mechanism underlying the effects of YLJP was verified in rats with precancerous lesions.

**Results:** The 1-year incidence of HCC was lower in the YLJP group than in the Western medicine group. The Wnt pathway protein, CTNNB1, is a key target of YLJP in preventing and treating HCC, and the canonical Wnt pathway is the key signaling pathway and is overexpressed in human liver tumors. In vivo experiments showed that YLJP significantly inhibited the canonical Wnt pathway and reduced the abnormal differentiation of hepatic oval cells. The binding of CTNNB1 to oleanolic acid, stigmasterol, and beta-sitosterol was found to be stable, indicating the action of these compounds in treating HCC.

**Conclusion:** YLJP reduces the 1-year incidence of HCC, with its mechanism likely due to oleanolic acid, beta-sitosterol, and stigmasterol inhibition of the CTNNB1 activation of the β-catenin protein, which in turn regulates the Wnt signaling pathway and prevents the abnormal differentiation of hepatic oval cells into cancer cells, thus delaying the occurrence and progression of the disease.

**Keywords:** network pharmacological analysis, molecular docking, molecular dynamics simulation, hepatocellular carcinoma, Wnt / β-catenin

## Introduction

Hepatocellular carcinoma (HCC) is the third most common cause of cancer death and is clinically characterized by high incidence and low survival.[1,2] Medical advancement has suggested that liver cirrhosis (LC) and abnormal alpha-fetoprotein (AFP) are risk factors for HCC,[3] and the nodular degeneration caused by LC has been considered a precancerous lesion.[4] Liver cancer is difficult to detect in its earliest stages; thus, the study of precancerous lesions has become a hot topic in the field of HCC prevention and treatment in recent years.

Received: 26 August 2024
Accepted: 12 November 2024
Published: 20 November 2024

Hepatic oval cells (HOCs) are considered to be progenitor cells of liver tumors, and the abnormal proliferation of HOC cells contributes to the development of liver malignancies.[5] HOCs are hepatic stem cells with bidirectional differentiation properties within the organism,[6] and will potentially transform into precancerous cells in the presence of persistent abnormal stimuli. HOCs also possess the tendency to develop into cancer cells, as seen in the precancerous liver cancer stage.[7,8] HCC is particularly vascular in terms of human cancers, and OV6 is a marker used to identify hematopoietic stem cells, with highly purified oval cell populations isolated using OV6.[9] CD34 is highly expressed on hematopoietic progenitor cells and is a surface marker of HOCs.[10] Among the many markers for vascular endothelial cells, CD34 is a sensitive and specific marker of the vascular changes that are associated with liver cancer.[11,12] Therefore, both OV6 and CD34 can be used to identify HOCs.

The canonical Wnt pathway activates gene transcription via the β-catenin protein (encoded by the proto-oncogene *CTNNB1*). Wnt1 and β-catenin are the key proteins of the canonical Wnt pathway.[13] Prior studies have revealed that both Wnt1 and β-catenin play an important role in the development of numerous cancers,[14,15] and an overactivated Wnt pathway has been found in many tumors, including liver and gastric cancers.[16,17] The Wnt pathway thus plays an important role in the occurrence and development of HCC, and studying the effector mechanism of this pathway for the treatment of precancerous lesions and prevention of HCC therefore provides a theoretical basis for the discovery of suitable HCC therapeutic targets.[18,19]

According to previous studies, abnormal activation of the Wnt pathway is inextricably linked to the development of HCC,[20,21] and traditional Chinese medicine (TCM) has been shown to have a significant regulatory effect on the Wnt pathway.[22–25] Yiqi Liangxue Jiedu prescription (YLJP) is a Chinese medicine used to prevent liver cancer and has been authorized by a national patent (No. ZL202110889980.5). YLJP is composed of 15 g *Adenophora stricta Miq*, 15 g *Ophiopogon japonicus*, 15 g *Codonopsis pilosula*, 15 g *Astragalus membranaceus*, 30 g *Hedyotis diffusa*, 15 g *Paris polyphylla*, 20 g *Atractylodes macrocephala*, 15 g *Wolfiporia extensa Ginns*, 9 g *Angelica sinensis*, and 15 g *Rehmannia glutinosa*. Exploring the mechanism of YLJP in the prevention of HCC can provide effective reference for the development of new drugs for the prevention and treatment of HCC.

# Material and Methods

## Study Materials and Methods

### Clinical Data and Samples

Liver cancer tumor tissues (n = 369) and normal tissues (n = 160) were obtained from the TCGA (https://www.cancer.gov/tcga) and GTEx (https://www.gtexportal.org/home/) databases, and R software (version 3.6.4) used to calculate the differences in gene expression between the normal and tumor tissues.

The clinical data of patients with hepatitis B-related precancerous lesions in cirrhosis with abnormal AFP from January 2015 to December 2020 were retrospectively collected at Beijing Ditan Hospital affiliated to Capital Medical University. Guidelines for the prevention and treatment of chronic hepatitis B (2015 version) were used as a reference for the diagnostic criteria of cirrhosis, and AFP ≥ 8.78ng/mL was considered abnormal (chemiluminescence microparticle immunoassay/Abbott Laboratories). The western medicine group was given ETV and TAF antiviral treatment, and compound glycyrrhizin and silymarin anti-inflammatory and liver-protecting treatment. Patients in the YLJP group were treated with oral YLJP decoction on the basis of western medicine treatment for a period of more than 3 months.

Human liver tissues, including cancer and para-cancer cirrhosis tissues, were obtained from 17 HCC patients between 2017 and 2018 at Beijing Ditan Hospital affiliated to Capital Medical University. This study was approved by the Ethics Committee of Beijing Ditan Hospital affiliated to Capital Medical University (Approval document NO.DTEC-KY2016-018-01).

## Experimental Methods and Data Analysis

### Animal Experiments

(1) Experimental Grouping. Thirty healthy male SD rats (SPF grade, 150 ± 10 g, 6-weeks-old) were purchased from SiPeiFu (Beijing) Biotechnology Co., LTD., China(Certificate No. SCXK (Beijing) 2019–0010), and randomly divided into three groups: control (10 rats), model (10 rats), and YLJP (10 rats).

(2) Experimental Procedures. Chinese medicines were purchased from Beijing Ditan Hospital Pharmacy. Herbs were ground into powder according to proportion and 450 mL water was added and stirred well, and then soaked for 30 min, boiled for 30 min, filtered, and stored at −80 °C. Rats in the model and YLJP groups were then administered 0.15 g/L 2-acetaminofluorene (2-AAF) via gavage for 1 week and subjected to 2/3 hepatectomies seven days later, according to the classical procedure. Administration was then suspended for three days following the hepatectomy, after which 0.15 g/L 2-AAF was administered via gavage for four weeks until the experiment was terminated at the end of week five. Gavage administration began at the same time as model construction in the model and YLJP groups, with 0.9 g/100 g administered to YLJP group rats (6.3 times the dosage administered to humans) via gavage (1 mL twice daily at 8 am and 5 pm). The model group was given normal saline and the YLJP group was given liquid containing the Chinese medicine. The control group was routinely administered with equal amounts of normal saline by gavage.

(3) Liver Processing. At the end of week five, rats were euthanized with intraperitoneal injection of 1% pentobarbital after 24 h of fasting. The residual liver was then rapidly removed and weighed, and liver tissue rapidly extracted from each rat. Tissues were fixed in 4% formaldehyde for paraffin embedding.

Routine pathological examinations, including hematoxylin and eosin staining and immunohistochemistry, were performed according to routine procedures.

All animal experiments were approved by the Animal Ethics Committee of Capital Medical University (approval document number: NO. AEEI-2023-200).

### Data Analysis

Experimental images were input into the medical image analysis system, and six liver tissue sections selected from each experimental group at 200× magnification for analysis, with five fields randomly observed in each section. The integrated optical density values of the brown-yellow positive particles in 30 fields were then calculated.

## Network Pharmacological Analysis and Enrichment Analysis of the KEGG Signaling Pathway

The compounds of the 10 herbs comprising the YLJP were obtained from the HERB database,[26] the SMILES string of compounds was obtained from the PubChem database,[27] and the relevant compound targets were further obtained from the Swiss Target Prediction database according to the SMILES string.[28] Targets related to LC and HCC were obtained from the DrugBank database.[29] The obtained YLJP, LC, and HCC targets were then intersected to obtain the potential therapeutic YLJP targets that may prevent the progression of liver precancerous lesions in HCC. A protein-protein interaction (PPI) network was then constructed among the intersected targets using the String database,[30] and Cytoscape software was used to construct and analyze the TCM-Compound-Target-HCC and PPI networks to obtain the key compounds and key targets in YLJP for the treatment of HCC.[31] Finally, KEGG pathway enrichment analysis was performed on the intersected targets in the Metascape database to identify the key signaling pathways of YLJP therapy for HCC.[32]

## Molecular Docking and Molecular Dynamics Simulation

The 3D structure of the protein was downloaded from the PDB database (http://www.rcsb.org/pdb/home/home.do) and the 2D structure of the compound from the TCMSP database (https://old.tcmsp-e.com/tcmsp.php). Both the protein and the compound structure were then processed by removing the water molecules, hydrogenation, and the addition of charges. Small molecular ligands were removed from the compound structure using MGLTools software and saved as PDBQT format files. AutoDock Vina software was used for molecular docking of the protein and compound structures, and Pymol software for 3D visualization.[33] The molecular dynamics of the protein receptor and complex ligand were simulated using GROMACS 2023 software (www.gromacs.org), and the ligand and receptor were parameterized using the Amber14SB force field. The complex was placed in a cube water box, solvated using the TIP3P water model, and 0.150 M of $Na^+$ and $Cl^-$ ions were added to neutralize the total charge. After energy minimization using the fastest descent method, equilibrium was carried out in 50,000 steps under NPT and NVT at a constant temperature and pressure of 310 K and 1 bar, respectively.

Unconstrained molecular dynamics simulation was then performed over 100 ns, with the energy and coordinate data of the system collected every 20 ns, and a total of 5000 frames of simulation trajectories were saved.

## Statistical Methods

SPSS 20.0 statistical software was used for statistical analysis. The paired *t*-test was used for normally distributed paired data and the nonparametric test for non-normally distributed paired data. Correlation tests for categorical data were performed using Spearman correlation, and the log-rank method was used to compare incidence. Differences of $p < 0.05$ were considered statistically significant.

# Results

## Treatment with YLJP Reduces the 1-Year HCC Incidence in Patients with Precancerous Liver Lesions

A total of 241 patients with cirrhosis combined with AFP who visited Beijing Ditan Hospital, Capital Medical University from 2015 to 2020 were included in the study, including 75 in the western medicine group and 166 in the YLJP group. The baseline patient data are presented in Table 1, the balance of clinical indexes between the two groups was comparable ($p > 0.05$). The K-M curves obtained for 1-year HCC incidence in the two groups are shown in Figure 1. The results showed significantly lower 1-year liver cancer incidence in the YLJP group that in the western medicine group ($p = 0.023$).

## Network Pharmacological Analysis Reveals the Wnt Signaling Pathway as the Key Pathway for YLJP in Preventing HCC

After analysis, 608 intersecting YJLP targets with both LC and HCC were obtained (Figure 2A). A total of 650 active compounds were observed in the 10 herbs of YLJP. Based on this, a TCM-Compound-Target-HCC complex network was constructed, topological analysis was performed, and the top 10 compounds in YLJP that are considered important for preventing and treating HCC were screened according to their degree value. A network diagram was then produced (Figure 2B), and 608 targets were used to build a PPI network (Figure 2C), which was subjected to topology analysis. The top 15 targets were then selected according to the degree value, and the key targets in YLJP for the prevention and treatment of HCC were obtained (Figure 2D). Finally, KEGG enrichment analysis was performed for the 608 targets, with the results again showing significant enrichment in the Wnt signaling pathway (hsa04310) for the YLJP targets (Figure 2E). It is worth noting that the Wnt signaling pathway-related gene, CTNNB1, is one of the 15 key targets of YLJP for the prevention and treatment of HCC.

**Table 1** Baseline Data for Chinese and Western Medicine Groups

| | **YLJP Group, (n=166)** | **Western Medicine Group (n=75)** | **P** |
|---|---|---|---|
| Gender (Male/ Female) | 115/51 | 46/29 | 0.226 |
| Age | 54.36±10.89 | 57.12±11.35 | 0.073 |
| Cr (umol/L) | 66.00 (39.00,119.90) | 63.80 (37.10,107.00) | 0.534 |
| ALT (U/L) | 33.35 (6.70, 340.30) | 30.60 (6.50, 271.40) | 0.254 |
| AST (U/L) | 39.05 (15.70,455.00) | 36.30 (15.90, 243.20) | 0.123 |
| TBIL (umol/L) | 20.70 (4.80, 351.70) | 18.50 (7.00,360.50) | 0.096 |
| DBIL (umol/L) | 8.85 (1.80, 280.20) | 8.10 (1.30, 274.30) | 0.183 |
| ALB (g/L) | 40.30 (20.30, 53.20) | 40.00 (23.80,49.20) | 0.466 |
| AFP (ng/mL) | 13.00 (1.50,1323.80) | 10.10 (2.00,997.10) | 0.189 |

**Notes**: YLJP, Yiqi Liangxue Jiedu prescription; Cr, creatinine; ALT, Alanine Transaminase; AST, Aspartate Aminotransferase; TBIL, Total Bilirubin; DBIL, Direct Bilirubin; ALB, Albumin; AFP, alpha-fetoprotein.

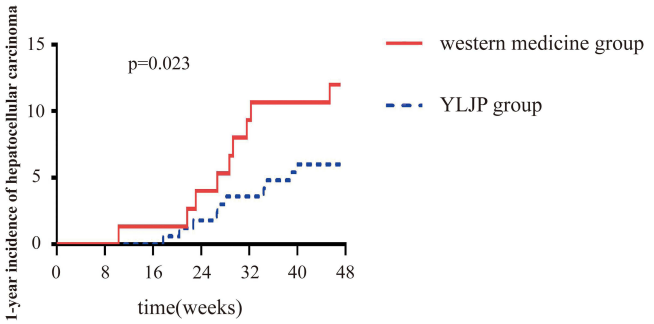


**Figure 1** One-year incidence of hepatocellular carcinoma (HCC) in both groups.

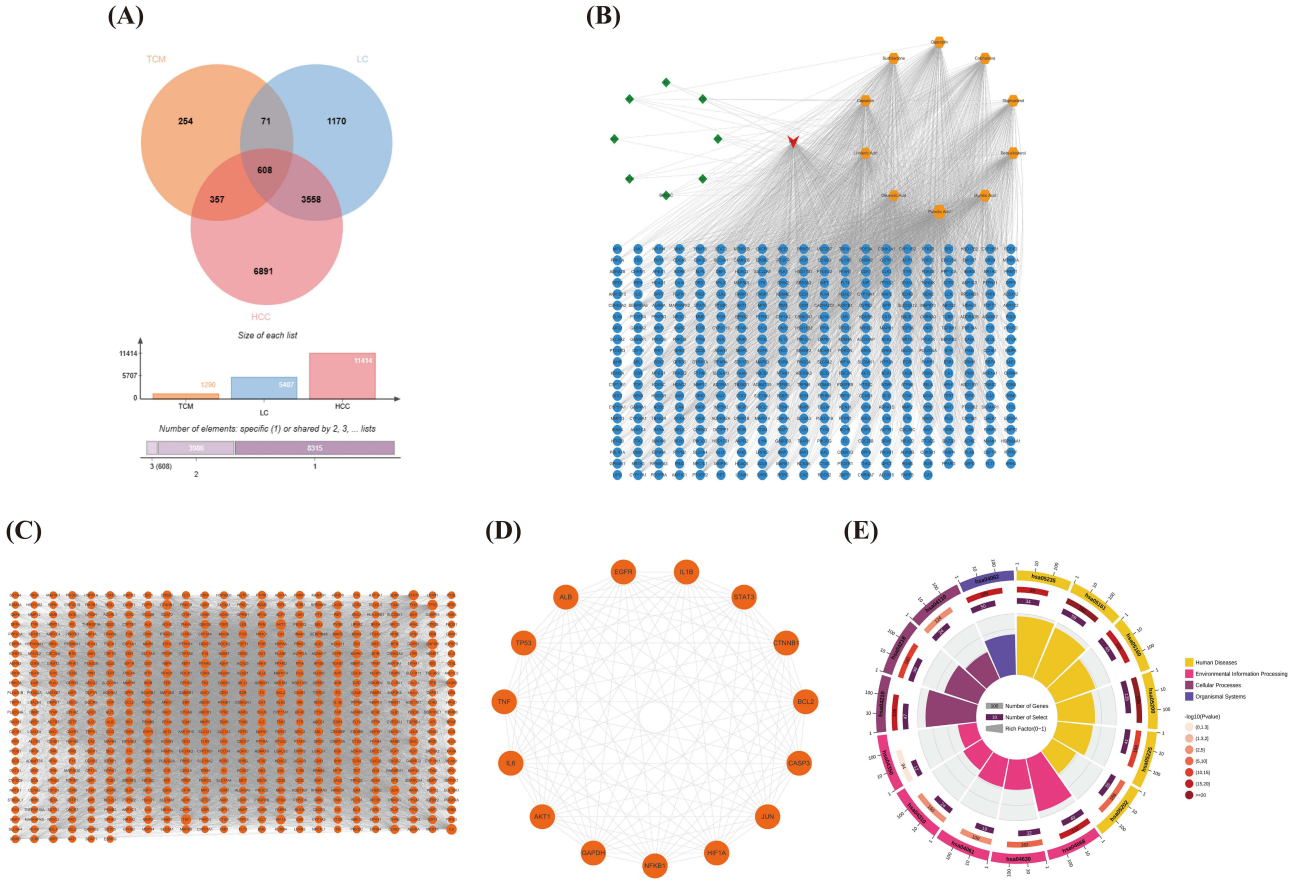


**Figure 2** Network pharmacology and KEGG analysis. (**A**) Intersection targets of traditional Chinese medicine(TCM), liver cirrhosis (LC) and hepatocellular carcinoma (HCC) (**B**) TCM - Compound - Target - HCC coincidence network. Blue nodes represent targets, Orange nodes represent 10 key compounds, green nodes represent traditional Chinese medicine (TCM), and red nodes represent hepatocellular carcinoma (HCC). (**C**) Protein-protein interaction (PPI) network. (**D**) Top 15 targets in the PPI network. (**E**) The 15 signaling pathways obtained in the results of KEGG pathway enrichment analysis.

# Molecular Docking and Molecular Dynamics Simulation Verifies Stable Binding Between the YLJP Compounds and the Wnt Pathway Protein CTNNB1

## Molecular Docking

Based on the results of the network pharmacological analysis, molecular docking was performed on the top 10 key compounds and 15 key targets of YLJP for the prevention and treatment of HCC. A binding energy of $\leq -5$ indicates stable binding between compound and target, and the results of the experiment indicated binding energy of $\leq -5$ for 82% of the compounds, suggesting good therapeutic effect for the compounds on most liver cancer targets (Figure 3A).

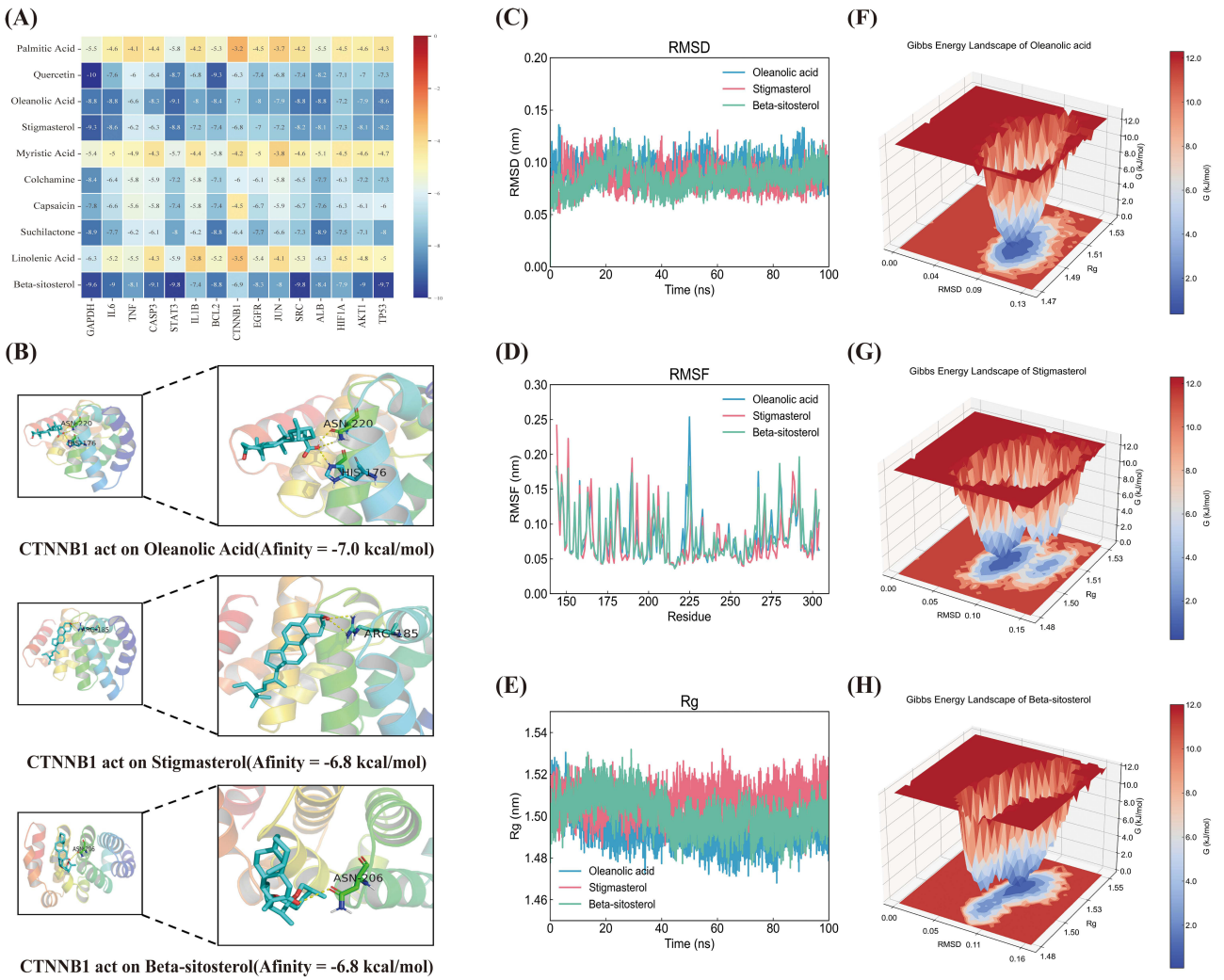


**Figure 3** Molecular docking and molecular dynamics simulation for CTNNB1 with oleanolic acid, stigmasterol, and beta-sitosterol. (**A**) Molecular docking binding energy scores for 15 compounds and 10 targets. (**B**) 3D simulation of molecular docking between CTNNB1 and oleanolic acid, stigmasterol, and beta-sitosterol. (**C**) RMSD diagram of CTNNB1 with oleanolic acid, stigmasterol, and beta-sitosterol. (**D**) RMSF diagram of CTNNB1 with oleanolic acid, stigmasterol, and beta-sitosterol. (**E**) Rg diagram of CTNNB1 with oleanolic acid, stigmasterol, and beta-sitosterol. (**F–H**) Gibbs energy landscape of CTNNB1-Oleanolic acid complexes, CTNBN1- Stigmasterol complexes and CTNBN1-Beta-Sitosterol complexes.

Considering that the Wnt signaling pathway protein CTNNB1 is one of the 15 key targets and the enrichment analysis results of the KEGG pathway suggest that Wnt signaling is an important signaling pathway for the prevention and treatment HCC when treating with YLJP. The binding stability between CTNNB1 and the 10 key compounds was focused upon, with results showing that oleanolic acid, stigmasterol, and beta-sitosterol were most strongly bound to CTNNB1. The docking of CTNNB1 with oleanolic acid, stigmasterol, and beta-sitosterol was then simulated in 3D, with results indicating that CTNNB1 binds to oleanolic acid via two amino acid residues (ASN-220 and HIS-176), to stigmasterol via one amino acid residue (ARG-185), and to beta-sitosterol via one amino acid residue (ASN-206) (Figure 3B).

## Molecular Dynamics Simulation

The binding affinity between CTNNB1 and oleanolic acid, stigmasterol, and beta-sitosterol was further verified using molecular dynamics simulation. RMSD curves can reflect the structural changes of proteins, and the RMSD values of the three pairs of complexes fluctuated in the range of 0.05–0.1 nm, with fluctuation values lower than 0.1 nm indicating normal fluctuation. This result indicates that the binding between the protein and the molecule was stabilized, and that the protein structure had reached a state of equilibrium (Figure 3C). The RMSF curve reflects the flexibility of amino acid

residues and the stability of the protein structure, and the RMSF curves obtained for the three pairs of complexes exhibited the same fluctuation trend. The RMSF value changed slightly, and the main fluctuation was concentrated from amino acid position 220 to amino acid position 228, within a randomly coiled segment (Figure 3D). The radius of gyration (Rg) is an important parameter in terms of protein conformation, with lower Rg values indicating higher spatial stability for a protein. The α-C atom of the amino acids in the three pairs of complexes fluctuated less during the simulation, indicating a particularly stable protein structure (Figure 3E). The Gibbs energy landscape shows changes in the conformational free energy of the protein during the simulation, with blue areas representing the energy centers. All three pairs of complexes had only one energy center and one major conformation (Figure 3F–H). Molecular dynamics simulations also showed that CTNNB1-Oleanolic acid, CTNNB1-Stigmasterol, and CTNNB1-Beta-sitosterol were stably bound.

## Aberrant Overexpression of the Canonical Wnt Pathway in Human Liver Cancer Tissues

Calculation of the difference between the expression of the Wnt pathway-related genes Wnt1 and CTNNB1 in liver cancer tumor tissues (n = 369) and normal tissues (n = 160) in the TCGA and GTEx databases indicated significant upregulation of Wnt1 and CTNNB1 in tumor tissues as compared to normal tissues (Figure 4A). Subsequently, the expression of the Wnt pathway-related proteins Wnt1 and β-catenin in the liver cancer tissues and cirrhotic tissues of 17 HCC patients were further examined, with the baseline data of the patients presented in Table 2. Most HCC cells were observed to be thin trabecular or pseudo-glandular, with polygons, abundant cytoplasm, eosinophilic round nuclei, visible

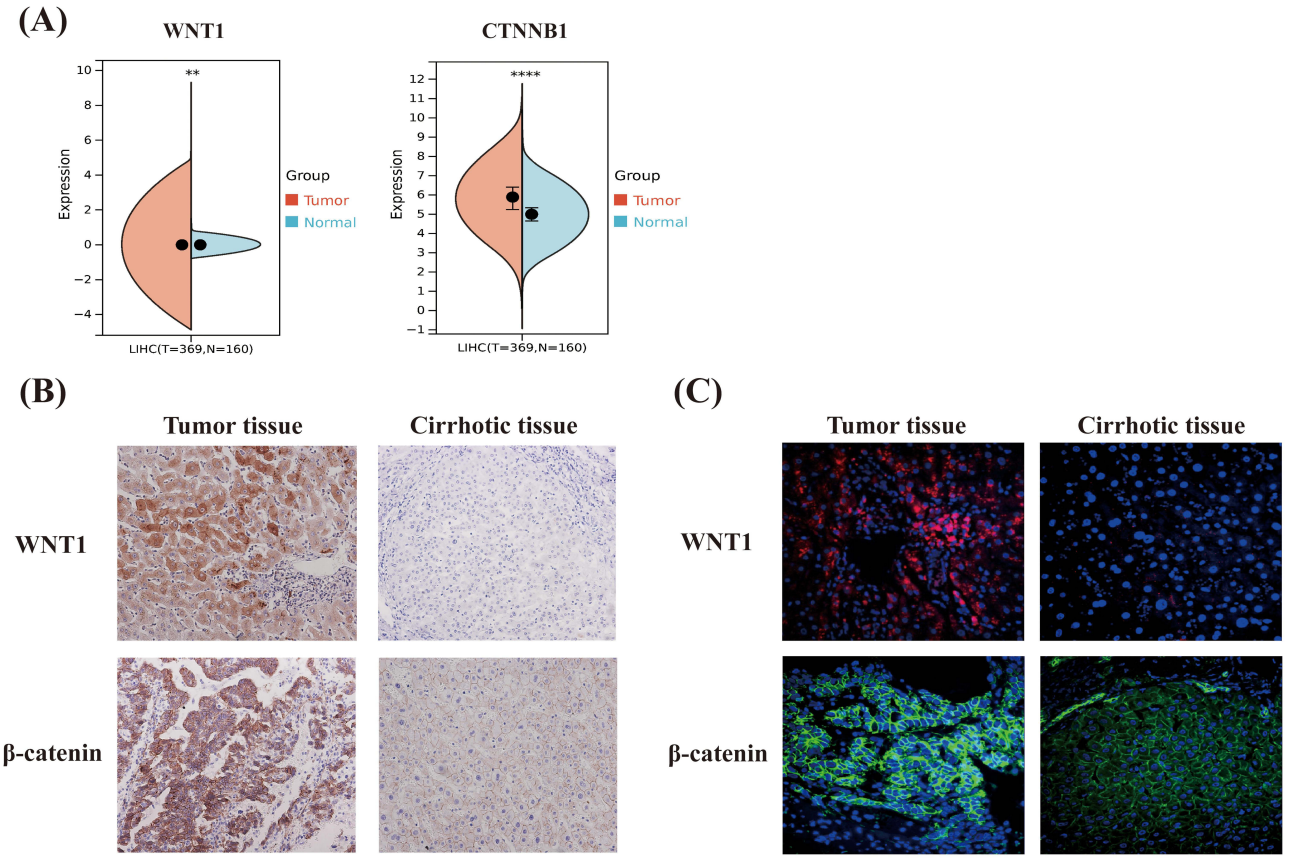


**Figure 4** Expression of Wnt1 and β-catenin was increased in hepatocellular carcinoma (HCC) tissues compared with normal tissues and cirrhotic tissues. (**A**) Wnt1 and CTNNB1 (encoding protein β-catenin) in liver cancer tumor tissues (n=369) and normal tissues (n=160) from the TCGA and GTEx databases, with**p < 0.01, ****p < 0.0001 compared to the normal group. (**B**) Expression of Wnt1 and β-catenin proteins in human liver tumor and cirrhotic tissues detected by immunohistochemistry (×200). (**C**) Expression of Wnt1 and β-catenin proteins in human liver tumor and cirrhotic tissues detected by immunofluorescence (×200).

**Table 2** Clinical Data of 17 Patients with Hepatocellular Carcinoma

| | Group | n |
|---|---|---|
| Age | ≥50 | 15 |
| | <50 | 2 |
| Sex | Male | 16 |
| | Female | 1 |
| HBsAg | ≥250 IU/mL | 9 |
| | <250 IU/mL | 8 |
| AFP | ≥400 ng/mL | 3 |
| | < 400 ng/mL | 14 |
| Pathological differentiation | Medium - high | 12 |
| | Low | 5 |
| Child-Pugh classification | A | 17 |
| | B | 0 |
| | C | 0 |
| BCLC | 0 | 0 |
| | A | 7 |
| | B | 7 |
| | C | 3 |
| | D | 0 |
| Chinese clinical stage | Ia | 4 |
| | Ib | 3 |
| | IIa | 3 |
| | IIb | 0 |
| | IIIa | 6 |
| | IIIb | 1 |
| | IV | 0 |

**Notes**: HBsAg, Hepatitis B surface antigen; AFP, alpha-fetoprotein; BCLC, Barcelona Clinic Liver Cancer.

nucleoli, and mild atypia. The intrahepatic mass did not invade the capsular membrane in most patients; however, a few masses invaded the subcapsule, and cirrhotic changes and a pseudo-lobular structure were observed in the surrounding liver tissues. Immunohistochemical and immunofluorescence detection results showed that the expression level of Wnt1 and β-catenin was significantly higher in the HCC tumor tissue group than in the paracancerous cirrhotic tissue group (Table 3, and Figure 4B and C), and the degree of pathological differentiation in patients with HCC was negatively correlated with β-catenin(with a Spearman correlation coefficient of −0.76, $p < 0.001$; Table 4), but the correlation between Wnt1 was not significant (Supplementary Table 1).

## YLJP Inhibits Liver Precancerous Lesions by Regulating the Wnt Pathway

### Histomorphological Structure of the Liver

The livers of rats in the control group displayed normal morphology, and were reddish-brown in color with a smooth, shiny surface and a soft texture. Under a light microscope, the hepatocytes were neatly arranged, polygonal or round, and

**Table 3** Immunohistochemical Staining of Wnt1 and β-Catenin in Liver Tissue of Different Groups of Patients

| | Tumor Tissues (n=17) | Cirrhotic Tissues (n=17) | P |
|---|---|---|---|
| Wnt1 | 30557.37 ± 9216.70 | 1026.04 ± 817.82 | < 0.001 |
| β-catenin | 22266.64 ± 7981.48 | 5825.15 ± 1942.49 | < 0.001 |

**Table 4** Analysis of the Correlation Between β-Catenin and Clinical Parameters in the Hepatocellular Carcinoma (HCC) Group

| Marker | Group | Mean ± Standard Deviation | Spearman Correlation Coefficient | P |
|---|---|---|---|---|
| AFP | ≤400 ng/mL | 21234.95±667.80 | 0.48 | 0.31 |
| | >400 ng/mL | 27081.21±13,347.82 | | |
| HBsAg | ≤250 IU/mL | 18821.20±1678.44 | −0.41 | 0.10 |
| | >250 IU/mL | 25329.26±3077.96 | | |
| Degree of differentiation | Medium - high | 18473.30±4047.16 | −0.76 | <0.001 |
| | Low | 31370.66±7937.25 | | |

**Note**: AFP, alpha-fetoprotein; HBsAg, hepatitis B surface antigen.

mostly mononuclear with basophilic nuclei located at the center of the cells. Slight eosinophilic cytoplasm was also observed, with the central vein at the center of the hepatic cord. The structure of the collecting duct was also visible (Figure 5A). In the model group, the structure of the liver tissue was disrupted, pseudolobules were observed, and some hepatocytes showed balloon-like changes, with large deeply stained nuclei, occasional nuclear division, and atypical proliferative changes. Several HOCs and inflammatory cells were found to have grown in the lobules, with collecting ducts at the center. HOCs appeared either round or oval in size and were smaller than normal hepatocytes, with large nuclei, visible nucleoli, basophilicity, and little cytoplasm (Figure 5B). The liver morphology of the YLJP group did not change significantly compared with that of the control group, which generally had a smooth and shiny surface and a soft texture, and was only occasionally enlarged and mildly congested. Under a light microscope, the structure of the liver lobules remained intact, and the few HOCs observed near the collecting ducts were smaller than normal hepatocytes. These cells appeared large, dark-stained, and possessed basophilic nuclei, visible nucleoli, little cytoplasm, and a high nucleoplasmic ratio (Figure 5C).

## Staining Results for HOC Markers OV6 and CD34

OV6: Microscopic analysis revealed a patchy yellow-brown-positive area near the collecting duct for the model group, representing cytoplasmic staining. The extent of the positive area and depth of staining were significantly reduced in the YLJP group and the control group showed negative results. Based on image analysis and statistical processing, OV6 expression was significantly lower in the YLJP group than the model group ($p < 0.01$) (Figure 6A–C and Table 5).

CD34: Based on microscopic analysis, the model group displayed dark brown staining near the collecting duct, with scattered staining observed in the hepatic lobules representing the cytoplasmic staining of hepatocytes or HOCs. The extent of the positivity and depth of the staining were reduced to varying degrees in the YLJP group. The control group

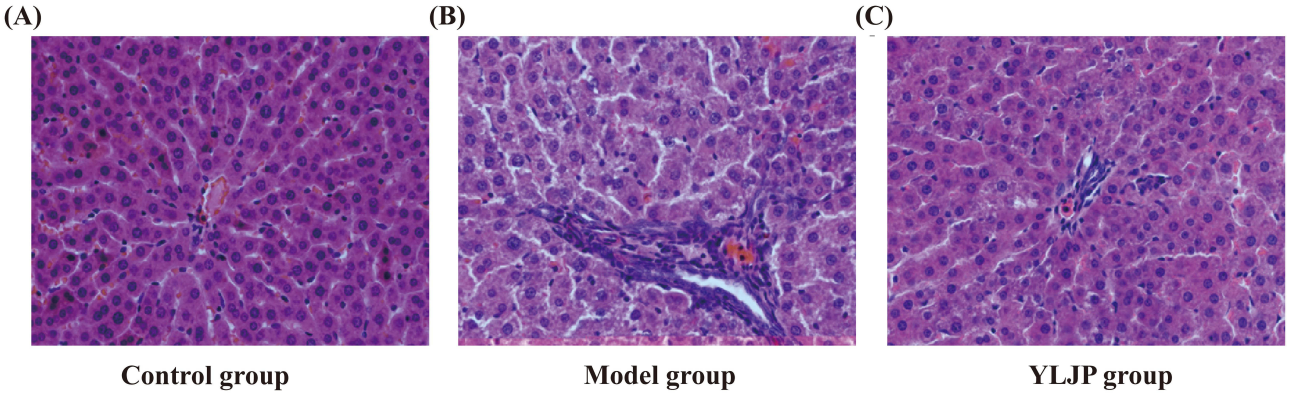


**Figure 5** HE staining of liver precancerous lesion model rat liver tissue (×400). (**A**) Control group. (**B**) Model group. (**C**) Yiqi Liangxue Jiedu prescription (YLJP) group.

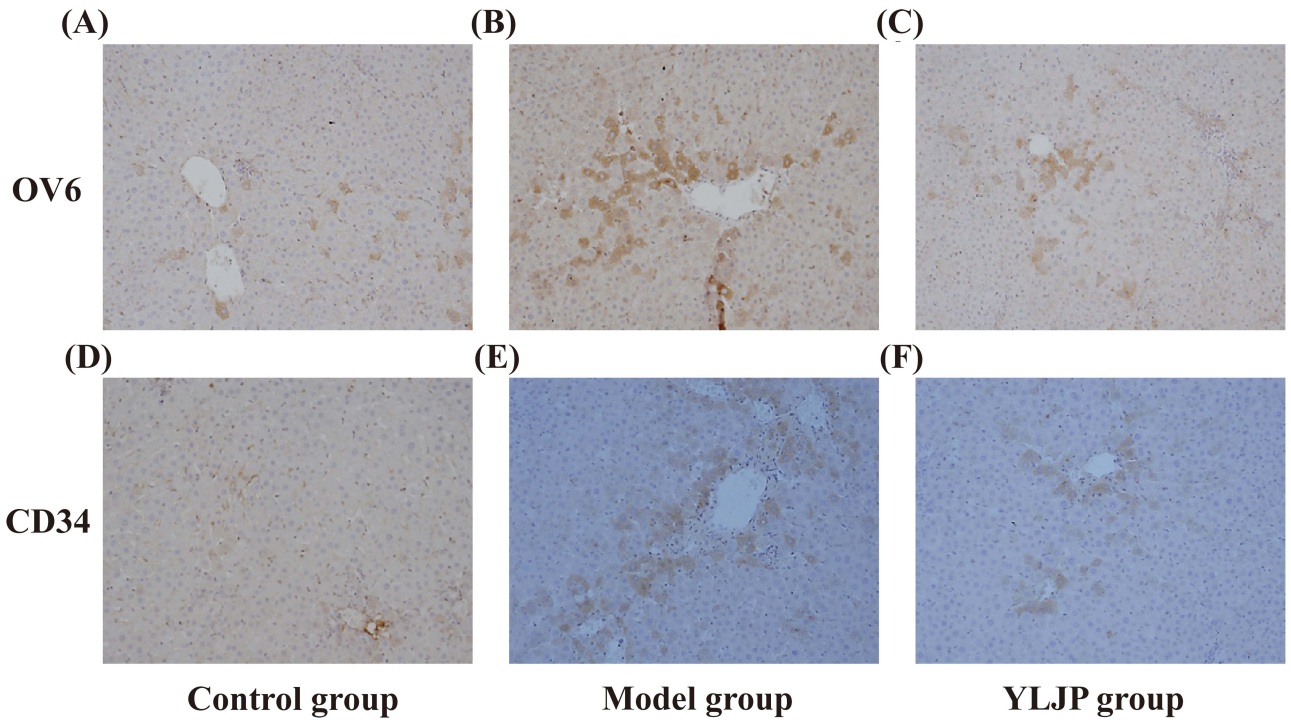


**Figure 6** Immunohistochemical staining of OV6 and CD34 in liver precancerous lesion model rat liver tissue (×200). (**A**–**C**) OV6 in control group, model group and Yiqi Liangxue Jiedu prescription (YLJP) group. (**D**–**F**) CD34 in control group, model group and Yiqi Liangxue Jiedu prescription (YLJP) group.

showed negative expression. According to image analysis and statistical processing, CD34 expression was significantly lower in the YLJP group as compared to the model group ($p < 0.01$) (Figure 6D–F and Table 5).

## Expression of the Wnt Pathway Key Proteins Wnt1 and β-Catenin

### Detection of Wnt1 and β-Catenin mRNA Expression Levels Using the RNAscope®2.5 Visible Light Dual-Staining Technique

Wnt1 mRNA molecules stained red, and expression was observed in the model group. Several mRNA molecules were visibly stained in the positive cells at 400× magnification, mainly near the collecting duct. These molecules also appeared as dotted red signals, were expressed in the cytoplasm and cell membrane, and were co-expressed in the same cells and nearby locations as β-catenin, which stained green. The semi-quantitative analysis method, which was performed according to the manufacturer's instructions, yielded scores of 1–3 for the model group. Positive staining was not observed in most cells of the control group, and a score of 0–1 was obtained. Few positive mRNA molecules were visible in some sections of the YLJP group, and 0–3 mRNA molecules stained positively within the positive cells at 400× magnification (score = 0–1). Co-staining of Wnt1 and β-catenin was observed in similar areas for all three groups. Nonparametric tests revealed a statistically significant difference between the model and control groups ($p < 0.01$) and the model and YLJP groups ($p < 0.05$). No significant differences were observed between the control and YLJP groups (Figure 7 and Table 6).

**Table 5** Immunohistochemical Staining of OV6 and CD34 in the Liver Tissues from Different Groups of Rats

| | Control Group (n=6) | Model Group (n=6) | YLJP Group (n=6) |
|---|---|---|---|
| OV6 | Negative | 22729.53±7812.89 | 9067.65±4884.15** |
| CD34 | Negative | 23555.21±14,743.52 | 5613.45±3022.24** |

**Notes**: Comparison with model group: **p< 0.01.

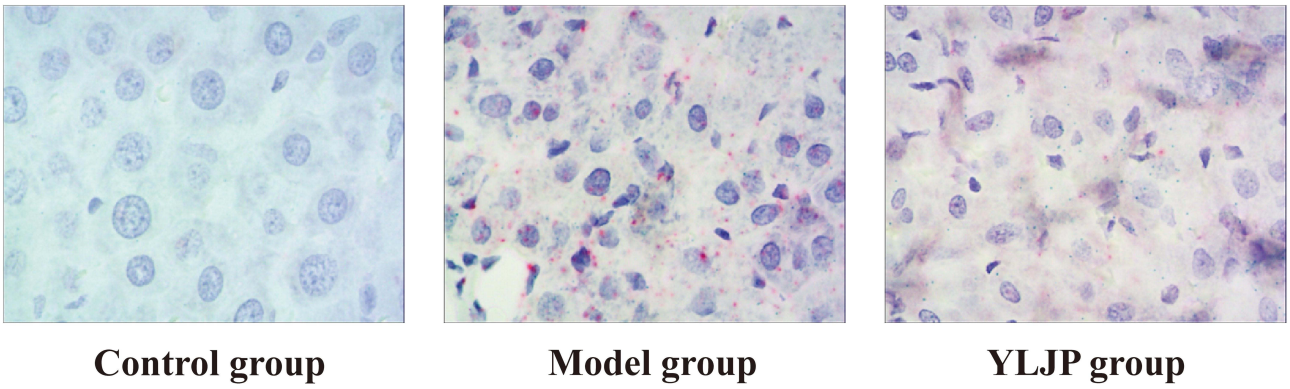


**Figure 7** mRNA expression of Wnt1 and β-catenin detected by In Situ Hybridization (ISH× 400).

β-catenin: mRNA molecules were stained green and were visible to some extent in the model group. However, the overall expression was higher than that of Wnt1. More than ten positive mRNA molecules were observed in the positive cells at 400× magnification; however, most did not display clustered staining signals, which were generally observed in the collecting duct or near the central vein, distributed in the cytoplasm and cell membrane, and were co-expressed with Wnt in the same location or neighboring regions (score = 2–4). Few positive mRNA molecules were occasionally observed in the control group; however, most sections were negative, with a score of 0–1. A total of 4–10 positively stained particles were observed in each positive cell in most sections of the YLJP group, and 1–3 positive signals were also observed; thus a score of 1–2 was calculated. Nonparametric tests revealed a statistically significant difference between the model and control groups ($p < 0.01$), and between the model and YLJP groups ($p < 0.05$). No significant differences were observed between the control and the YLJP groups (Figure 7 and Table 6).

### Immunohistochemical Detection of Wnt1 and β-Catenin Protein Expression

Wnt1. The cytoplasm and cytosol of several hepatocytes and HOCs in the model group stained brownish yellow were located near the collecting duct and scattered throughout the liver tissue. Positive cells had larger and darker nuclei, smaller cell volumes, and relatively less cytoplasm than normal hepatocytes. Few positive or negative cells were observed in the control group, and few positive cells were observed near the collecting duct in the YLJP group.

**Table 6** In situ Hybridization Staining of Wnt1 and β-Catenin in Liver Tissues from the Different Groups of Rats

| | Point | Control Group, n=6 (%) | Model Group, n=6 (%) | YLJP Group, n=6 (%) |
|---|---|---|---|---|
| Wnt1 | | ** | – | * |
| | 0 | 5 (83.3%) | 0 | 3(50.0%) |
| | 1 | 1(16.7%) | 1 (16.7%) | 2(33.3%) |
| | 2 | 0 | 3 (50.0%) | 0 |
| | 3 | 0 | 2 (33.3%) | 1 (16.7%) |
| | 4 | 0 | 0 | 0 |
| β-catenin | | ** | - | * |
| | 0 | 5 (83.3%) | 0 | 0 |
| | 1 | 1(16.7%) | 0 | 4(66.7%) |
| | 2 | 0 | 3(50.0%) | 2(33.3%) |
| | 3 | 0 | 2(33.3%) | 0 |
| | 4 | 0 | 1 (16.7%) | 0 |

**Notes**: Comparison with model group: *p< 0.05, **p< 0.01.

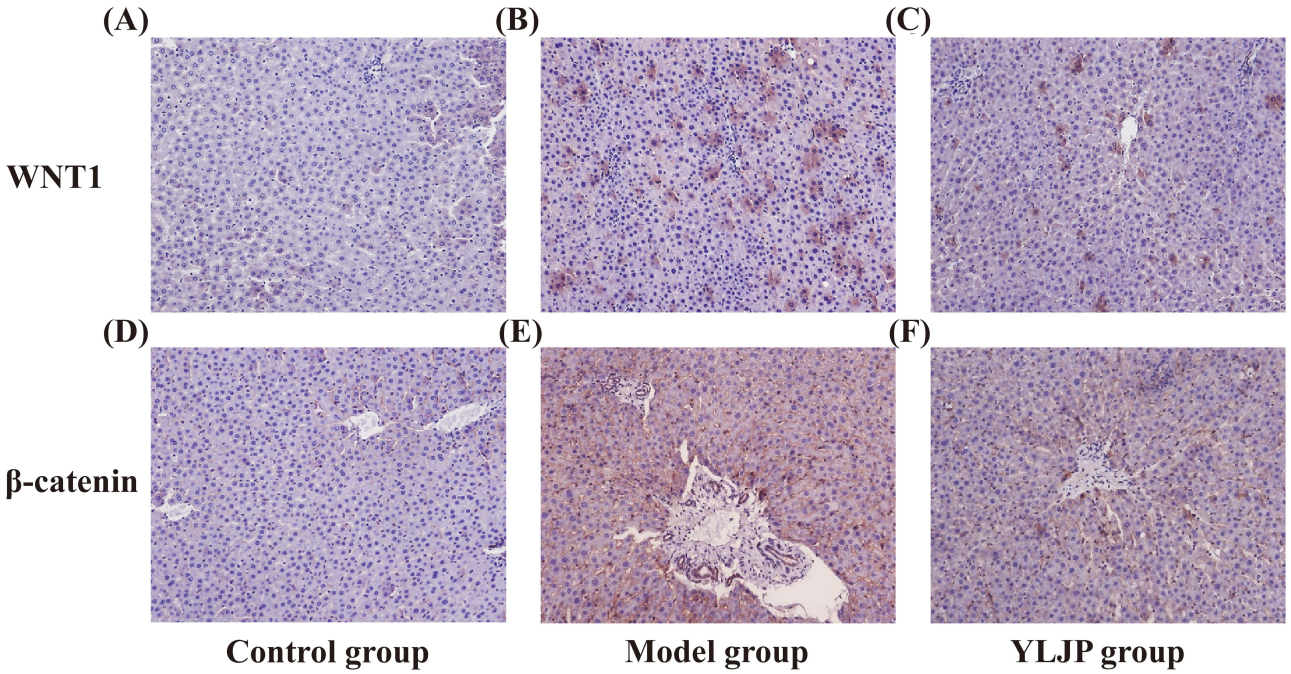


**Figure 8** Immunohistochemical staining of Wnt1 and β-catenin (IHC × 200). (**A**–**C**) Wnt1 in control group, model group, and Yiqi Liangxue Jiedu prescription (YLJP) group. (**D**–**F**) β-catenin in control group, model group, and Yiqi Liangxue Jiedu prescription (YLJP) group.

Significant differences were observed between the model and the control and between the model and YLJP ($p < 0.01$), however, the differences between the YLJP and control were not significant (Figure 8A–C and Table 7).

β-Catenin. Several positive areas were observed in the cytoplasm. Furthermore, the cell membrane was observed near the collecting duct and scattered in the liver tissue in the model group. Few positive or negative cells were observed in the control group, and fewer positive areas concentrated near the collecting duct were observed in the YLJP group. Significant differences were observed between the model and control and between the model and YLJP ($p < 0.01$), however, the differences between YLJP and the control were not significant (Figure 8D–F and Table 7).

## Discussion

According to WHO statistics, approximately 1 million people die from infectious severe liver disease every year, with an average of 2 deaths every minute, of which hepatitis B liver cancer accounts for the largest proportion. Liver cancer mortality rate ranks third in the world, and the five-year survival rate of liver cancer is only 12.1%.[1,2] A high percentage (70%) of liver cancer patients are in the unresectable middle and late stages when they are first diagnosed, losing the opportunity for surgical treatment.[34] Therefore, the early diagnosis and treatment or prevention of liver cancer are particularly important. TCM and modern Chinese medicine preparations can be used for conversion and conservative treatments in all stages of liver cancer; thus, TCM is an important means of preventing and treating liver cancer.

YLJP is a Chinese medicine used for the prevention of liver cancer that has obtained a national patent certification (Patent No. ZL202110889980.5). In this study, retrospective analysis of the 1-year incidence of HCC in 241 patients with

**Table 7** Immunohistochemical Staining of Wnt1 and β-Catenin in the Liver Tissues from Different Groups of Rats

| | Control Group (n=6) | Model Group (n=6) | YLJP Group (n=6) |
|---|---|---|---|
| Wnt1 | 4943.77±816.42** | 8499.95±5098.58 | 5851.96±2002.90** |
| β-catenin | 2600.69±1438.03** | 27,449.01±2775.57 | 5993.25±1583.51** |

**Notes**: Comparison with model group: **p< 0.01.

cirrhosis with abnormal AFP confirmed that YLJP can indeed reduce the 1-year incidence of HCC in these patients. In recent years, network pharmacological analysis has been widely used for the discovery of active compounds in TCM and the interpretation of overall mechanisms of action. In this study, network pharmacological analysis indicated that the mechanism of action of YLJP is significantly related to the Wnt signaling pathway, the Wnt signaling pathway gene *CTNNB1* is an important therapeutic target. Molecular docking results showed that most key YLJP compounds were stably bound to CTNNB1, with oleanolic acid, beta-sitosterol, and stigmasterol demonstrated the strongest binding. Molecular simulation revealed stable binding of CTNNB1-Oleanolic acid, CTNNB1-Stigmasterol, and CTNNB1-Beta-sitosterol.

Molecular dynamics simulation results show that CTNNB1-Oleanolic acid, CTNNB1-Stigmasterol, and CTNNB1-Beta-sitosterol have a high affinity. *CTNNB1* mutations lead to larger tumors in HCC patients when activated by beta-catenin, and that microscopic vascular invasion, tumor capsule invasion, and intratumor cholestasis are more likely to occur.[35] Oleanolic acid, beta-sitosterol, and stigmasterol alone or in combination with sorafenib can reduce tumor volume and inhibit HCC progression.[36–38] Several studies have shown that oleanolic acid and beta-sitosterol can regulate the Wnt/β-catenin pathway and reduce the expression of β-catenin protein (encoded by *CTNNB1*).[39–41] Previous studies and the results of this study suggest that YJLP may inhibit the CTNNB1 activation of the β-catenin protein through the actions of oleanolic acid, beta-sitosterol, and stigmasterol, thereby regulating the Wnt signaling pathway and delaying the occurrence and progression of HCC.

To explore the role of canonical Wnt pathways in the occurrence and development of liver cancer, the differences in the expression of Wnt pathway key molecules, Wnt1 and CTNNB1, between liver tumors and normal tissues from the public databases TCGA and GTEx were analyzed, with results showing significantly higher Wnt1 and CTNNB1 expression in tumor tissues compared with those in normal tissues. The same phenomenon was also observed in the tumor and cirrhosis tissues of 17 HCC patients, with significant upregulation of Wnt1 and β-catenin in the tumor tissues. It was also observed that Wnt1 was mainly present in the cytoplasm, while β-catenin was also present in the cell membrane, cytoplasm, and nucleus. Previous studies have shown that Wnt-1 is highly expressed in human liver cancer cell lines and human HCC tissues, while Wnt1 and β-catenin are significantly up-regulated in non-small cell lung cancer and colon cancer tissues as compared with normal tissues.[42–44] Xu et al found that Wnt1 expression appeared in the form of cytoplasmic staining pattern in non-small cell lung cancer tumor tissues and that β-catenin expression was localized in the membrane of normal epithelial cells; however, the expression was reduced in the membrane and cytoplasmic expression and/or nuclear translocation occurred.[45] The above results are highly consistent with our own, suggesting that the Wnt pathway is abnormally activated during the progression of liver cancer from precancerous lesion to liver cancer.

We further used YLJP to treat precancerous liver cancer model rats and measured the mRNA and protein levels of Wnt1 and CTNNB1 to verify whether YLJP has a regulatory effect on the canonical Wnt pathway. Compared with the control, the mRNA and protein expressions of Wnt1 and β–catenin in the model group were significantly increased, indicating activation of the canonical Wnt pathway in rats with precancerous liver lesions, which is consistent with the results obtained using data from the public database and clinical sample analysis. After intervention with YLJP, the expressions of Wnt1 and β-catenin in YLJP group were significantly decreased compared with those in the model group, and no significant difference was observed between the YLJP group and the control, indicating that YLJP can significantly reduce the expressions of Wnt1 and β-catenin in the liver tissues of precancerous model rats. These findings suggest that YLJP has a significant regulatory effect on the canonical Wnt pathway, and the molecular mechanism underlying its prevention and treatment may involve inhibition of the canonical Wnt pathway. Based on an experiment on rats with precancerous lesions, multiple clusters of OV6 and CD34 positive hepatocytes were found in the liver tissues of rats with precancerous lesions, suggesting abundant abnormal HOC proliferation in the liver tissues of the model rats. HOCs in the liver tissues of the model rats were transformed into precancerous cells and cancer cells under continuous abnormal stimulation, gradually developing into HCC. OV6 and CD34 expression in the liver tissue of model rats was significantly reduced under YLJP treatment, indicating a decrease in the number of HOCs. Experiments have shown that YLJP can block precancerous hepatocellular lesions by inhibiting HOC carcinogenesis.

## Conclusion

In this study, YLJP was found capable of reducing the 1-year incidence of HCC, likely through mechanisms associated with inhibition of CTNNB1 activation of β-catenin protein through the actions of oleanolic acid, beta-sitosterol, and stigmasterol, which regulate the Wnt signaling pathway and prevent the abnormal differentiation of normal HOCs into cancer cells, delaying the occurrence and progression of HCC. Our study provides a new perspective for the prevention and treatment of HCC and a reliable reference for the development of new drugs. In conclusion, the selective inhibition of the Wnt pathway activation in the precancerous stage of HCC may be a promising therapeutic strategy.

Some limitations are associated with this study. First, we demonstrated only that CTNNB1 could stably bind to oleanolic acid, beta-sitosterol, and stigmasterol. However, the effects of oleanolic acid, beta-sitosterol, and stigmasterol on the expression level of CTNNB1 were not verified. Second, YLJP can prevent the abnormal differentiation of normal HOCs into cancer cells and has a significant inhibitory effect on the canonical WNT pathway. However, whether YLJP prevents the abnormal differentiation of normal HOCs into cancer cells by inhibiting the canonical Wnt pathway requires further investigation.

## Abbreviations

YLJP, Yiqi Liangxue Jiedu prescription; HCC, hepatocellular carcinoma; LC, liver cirrhosis; AFP, alpha-fetoprotein; HOCs: Hepatic oval cells; TCM, traditional Chinese medicine; PPI, protein-protein interaction; 2-AAF, 2-acetamino-fluorene; K-M curves, Kaplan-Meier curves.

## Data Sharing Statement

The datasets generated and/or analyzed in the current study are available from the corresponding author upon reasonable request.

## Ethics Approval and Consent to Participate

All data from TCGA and GTEx are free and open-source data, legally obtained in accordance with TCGA and GTEx Data access policies and published manuals; therefore, this part of the study does not require ethical review by the Ethical Review Committee of the hospital. As the clinical data of 241 patients were retrospective, the hospital ethics committee exempted us from ethical review. The clinical liver tissue samples collected in this study were carried out in accordance with the Declaration of Helsinki and approved by the Ethics Committee of Beijing Ditan Hospital, Capital Medical University (Approval document NO.DTEC-KY2016-018-01). All patients participating in this study signed an informed consent for their data to be used in this study. All animal experiments were approved by the Animal Ethics Committee of Capital Medical University (approval document number: NO. AEEI-2023-200), in strict abidance with the “Five F” and “Three R” principles, and were performed following the Guide for the Care and Use of Laboratory Animals of the National Institutes of Health, USA.

## Acknowledgments

We acknowledge and appreciate the valuable suggestions and technical assistance of our colleagues in this study.

## Author Contributions

All authors made a significant contribution to the work reported, whether that is in the conception, study design, execution, acquisition of data, analysis and interpretation, or in all these areas; took part in drafting, revising or critically reviewing the article; gave final approval of the version to be published; have agreed on the journal to which the article has been submitted; and agree to be accountable for all aspects of the work.

## Funding

This study was supported by the National Science Foundation of China (No. 82274479), the High-level Public Health Technical Personnel Construction Project (Subject leaders-02-16), the Dengfeng Talent Support Program from the

Beijing Municipal Administration of Hospitals (No. DFL20191803), the Beijing Hospital Authority Clinical Medicine Development with Special Funding Support (No. ZYLX202127), Special Fund of Capital Health Research and Development (No. 2020-2-2173), and the Beijing Municipal Science and Technology Commission (No. Z171100001017082).

## Disclosure

Dr Zhibo Dang reports a patent A traditional Chinese medicine composition for preventing liver cancer and its application (NO.ZL202110889980.5) issued to Zhiyun Yang; Dr Lihua Yu reports a patent A traditional Chinese medicine composition for preventing liver cancer and its application (NO.ZL202110889980.5) issued to Zhiyun yang. The authors declare no other competing interests in this work.

## References

1. Rumgay H, Arnold M, Ferlay J, et al. Global burden of primary liver cancer in 2020 and predictions to 2040. *J Hepatol*. 2022;77(6):1598–1606. doi:10.1016/j.jhep.2022.08.021
2. Zeng H, Chen W, Zheng R, et al. Changing cancer survival in China during 2003-15: a pooled analysis of 17 population-based cancer registries. *Lancet Glob Health*. 2018;6(5):e555–e567. doi:10.1016/S2214-109X(18)30127-X
3. Yang JD, Hainaut P, Gores GJ, Amadou A, Plymoth A, Roberts LR. A global view of hepatocellular carcinoma: trends, risk, prevention and management. *Nat Rev Gastroenterol Hepatol*. 2019;16(10):589–604. doi:10.1038/s41575-019-0186-y
4. Desjonqueres E, Campani C, Marra F, Zucman-Rossi J, Nault JC. Preneoplastic lesions in the liver: molecular insights and relevance for clinical practice. *Liver Int*. 2022;42(3):492–506. doi:10.1111/liv.15152
5. Li CH, Wang YJ, Dong W, et al. Hepatic oval cell lines generate hepatocellular carcinoma following transfection with HBx gene and treatment with aflatoxin B1 in vivo. *Cancer Lett*. 2011;311(1):1–10. doi:10.1016/j.canlet.2011.05.035
6. Sell S, Leffert HL. Liver cancer stem cells. *J Clin Oncol*. 2008;26(17):2800–2805. doi:10.1200/JCO.2007.15.5945
7. Libbrecht L, Roskams T. Hepatic progenitor cells in human liver diseases. *Semin Cell Dev Biol*. 2002;13(6):389–396. doi:10.1016/S1084952102001258
8. Zheng T, Wang J, Jiang H, Liu L. Hippo signaling in oval cells and hepatocarcinogenesis. *Cancer Lett*. 2011;302(2):91–99. doi:10.1016/j.canlet.2010.12.008
9. Yang L, Li S, Hatch H, et al. In vitro trans-differentiation of adult hepatic stem cells into pancreatic endocrine hormone-producing cells. *Proc Natl Acad Sci U S A*. 2002;99(12):8078–8083. doi:10.1073/pnas.122210699
10. Facciorusso A, Antonino M, Del Prete V, Neve V, Scavo MP, Barone M. Are hematopoietic stem cells involved in hepatocarcinogenesis? *Hepatobiliary Surg Nutr*. 2014;3(4):199–206. doi:10.3978/j.issn.2304-3881.2014.06.02
11. Frachon S, Gouysse G, Dumortier J, et al. Endothelial cell marker expression in dysplastic lesions of the liver: an immunohistochemical study. *J Hepatol*. 2001;34(6):850–857. doi:10.1016/S0168-8278(01)00049-6
12. Pang R, Poon RT. Angiogenesis and antiangiogenic therapy in hepatocellular carcinoma. *Cancer Lett*. 2006;242(2):151–167. doi:10.1016/j.canlet.2006.01.008
13. MacDonald BT, Tamai K, He X. Wnt/beta-catenin signaling: components, mechanisms, and diseases. *Dev Cell*. 2009;17(1):9–26. doi:10.1016/j.devcel.2009.06.016
14. Xu T, Zeng Y, Shi L, et al. Targeting NEK2 impairs oncogenesis and radioresistance via inhibiting the Wnt1/β-catenin signaling pathway in cervical cancer. *J Exp Clin Cancer Res*. 2020;39(1):183. doi:10.1186/s13046-020-01659-y
15. Li Y, Wang Y, Zou Q, Li S, Zhang F. KLF3 Transcription Activates WNT1 and Promotes the Growth and Metastasis of Gastric Cancer via Activation of the WNT/β-Catenin Signaling Pathway. *Lab Invest*. 2023;103(6):100078.
16. Mao T, Chu J, Jeng Y, et al. Expression of mutant nuclear β-catenin correlates with non-invasive hepatocellular carcinoma, absence of portal vein spread, and good prognosis. *J Pathol*. 2015;193(1):95–101. doi:10.1002/1096-9896(2000)9999:9999<::AID-PATH720>3.0.CO;2-3
17. Woo DK, Kim HS, Lee HS, et al. Altered expression and mutation of β-catenin gene in gastric carcinomas and cell lines. *Int J Cancer*. 2001;95(2):108–113.
18. Perugorria MJ, Olaizola P, Labiano I, et al. Wnt–β-catenin signalling in liver development, health and disease. *Nat Rev Gastroenterol Hepatol*. 2019;16(2):121–136. doi:10.1038/s41575-018-0075-9
19. Anastas JN, Moon RT. WNT signalling pathways as therapeutic targets in cancer. *Nat Rev Cancer*. 2013;13(1):11–26. doi:10.1038/nrc3419
20. Zou G, Park JI. Wnt signaling in liver regeneration, disease, and cancer. *Clin Mol Hepatol*. 2023;29(1):33–50. doi:10.3350/cmh.2022.0058
21. Russell JO, Monga SP. Wnt/β-Catenin Signaling in Liver Development, Homeostasis, and Pathobiology. *Annu Rev Pathol*. 2018;13(1):351–378. doi:10.1146/annurev-pathol-020117-044010
22. Yang Z, Zhang Q, Yu L, Zhu J, Cao Y, Gao X. The signaling pathways and targets of traditional Chinese medicine and natural medicine in triple-negative breast cancer. *J Ethnopharmacol*. 2021;264:113249. doi:10.1016/j.jep.2020.113249
23. Wu XL, Lin SG, Mao YW, et al. Wnt/β-catenin signalling pathway in breast cancer cells and its effect on reversing tumour drug resistance by alkaloids extracted from traditional Chinese medicine. *Expert Rev Mol Med*. 2023;25:e21.
24. Dai X, Liu Y, Liu T, et al. SiJunZi decoction ameliorates bone quality and redox homeostasis and regulates advanced glycation end products/receptor for advanced glycation end products and WNT/β-catenin signaling pathways in diabetic mice. *J Ethnopharmacol*. 2024;319(Pt 2):117167. doi:10.1016/j.jep.2023.117167
25. Xia H, Cao D, Yang F, et al. Jiawei Yanghe decoction ameliorates cartilage degradation in vitro and vivo via Wnt/β-catenin signaling pathway. *Biomed Pharmacother*. 2020;122:109708. doi:10.1016/j.biopha.2019.109708

26. Fang S, Dong L, Liu L, et al. HERB: a high-throughput experiment- and reference-guided database of traditional Chinese medicine. *Nucleic Acids Res*. 2021;49(D1):D1197–D1206. doi:10.1093/nar/gkaa1063
27. Kim S, Chen J, Cheng T, et al. PubChem in 2021: new data content and improved web interfaces. *Nucleic Acids Res*. 2021;49(D1):D1388–D1395. doi:10.1093/nar/gkaa971
28. Gfeller D, Grosdidier A, Wirth M, Daina A, Michielin O, Zoete V. SwissTargetPrediction: a web server for target prediction of bioactive small molecules. *Nucleic Acids Res*. 2014;42(Web Server issue):W32–W38. doi:10.1093/nar/gku293
29. Wishart DS, Feunang YD, Guo AC, et al. DrugBank 5.0: a major update to the DrugBank database for 2018. *Nucleic Acids Res*. 2018;46(D1):D1074–D1082. doi:10.1093/nar/gkx1037
30. Szklarczyk D, Kirsch R, Koutrouli M, et al. The STRING database in 2023: protein-protein association networks and functional enrichment analyses for any sequenced genome of interest. *Nucleic Acids Res*. 2023;51(D1):D638–D646. doi:10.1093/nar/gkac1000
31. Shannon P, Markiel A, Ozier O, et al. Cytoscape: a software environment for integrated models of biomolecular interaction networks. *Genome Res*. 2003;13(11):2498–2504. doi:10.1101/gr.1239303
32. Zhou Y, Zhou B, Pache L, et al. Metascape provides a biologist-oriented resource for the analysis of systems-level datasets. *Nat Commun*. 2019;10(1):1523. doi:10.1038/s41467-019-09234-6
33. Kitchen DB, Decornez H, Furr JR, Bajorath J. Docking and scoring in virtual screening for drug discovery: methods and applications. *Nat Rev Drug Discov*. 2004;3(11):935–949. doi:10.1038/nrd1549
34. Zhang W, Tong S, Hu B, et al. Lenvatinib plus anti-PD-1 antibodies as conversion therapy for patients with unresectable intermediate-advanced hepatocellular carcinoma: a single-arm, Phase II trial. *J Immunother Cancer*. 2023;11(9):e007366. doi:10.1136/jitc-2023-007366
35. Wei W, Chua MS, Grepper S, So SK. Blockade of Wnt-1 signaling leads to anti-tumor effects in hepatocellular carcinoma cells. *Mol Cancer*. 2009;8(1):76. doi:10.1186/1476-4598-8-76
36. Rebouissou S, Franconi A, Calderaro J, et al. Genotype-phenotype correlation of CTNNB1 mutations reveals different ß-catenin activity associated with liver tumor progression. *Hepatology*. 2016;64(6):2047–2061. doi:10.1002/hep.28638
37. Lange M, Abhari BA, Hinrichs TM, Fulda S, Liese J. Identification of a novel oxidative stress induced cell death by Sorafenib and oleanolic acid in human hepatocellular carcinoma cells. *Biochem Pharmacol*. 2016;118:9–17. doi:10.1016/j.bcp.2016.08.011
38. Huo R, Yang WJ, Liu Y, et al. Stigmasterol: remodeling gut microbiota and suppressing tumor growth through Treg and CD8+ T cells in hepatocellular carcinoma. *Phytomedicine*. 2024;129:155225. doi:10.1016/j.phymed.2023.155225
39. Ma T, Ruan H, Lv L, et al. Oleanolic acid, a small-molecule natural product, inhibits ECM degeneration in osteoarthritis by regulating the Hippo/YAP and Wnt/β-catenin pathways. *Food Funct*. 2023;14(22):9999–10013. doi:10.1039/D3FO01902K
40. Chen Y, Yang Y, Wang N, et al. β-Sitosterol suppresses hepatocellular carcinoma growth and metastasis via FOXM1-regulated Wnt/β-catenin pathway. *J Cell Mol Med*. 2024;28(3):e18072. doi:10.1111/jcmm.18072
41. Gu S, Liu F, Xie X, et al. β-Sitosterol blocks the LEF-1-mediated Wnt/β-catenin pathway to inhibit proliferation of human colon cancer cells. *Cell Signal*. 2023;104:110585. doi:10.1016/j.cellsig.2022.110585
42. Chen Y, Yin S, Liu R, et al. β-Sitosterol activates autophagy to inhibit the development of hepatocellular carcinoma by regulating the complement C5a receptor 1/alpha fetoprotein axis. *Eur J Pharmacol*. 2023;957:175983. doi:10.1016/j.ejphar.2023.175983
43. Cui G, Fu X, Wang W, et al. LINC00476 Suppresses the Progression of Non-Small Cell Lung Cancer by Inducing the Ubiquitination of SETDB1. *Radiat Res*. 2021;195(3):275–283. doi:10.1667/RADE-20-00105.1
44. Li B, Shi C, Li B, Zhao JM, Wang L. The effects of Curcumin on HCT-116 cells proliferation and apoptosis via the miR-491/PEG10 pathway. *J Cell Biochem*. 2018;119(4):3091–3098. doi:10.1002/jcb.26449
45. Xu X, Sun PL, Li JZ, Jheon S, Lee CT, Chung JH. Aberrant Wnt1/β-catenin expression is an independent poor prognostic marker of non-small cell lung cancer after surgery. *J Thorac Oncol*. 2011;6(4):716–724. doi:10.1097/JTO.0b013e31820c5189